spectroscopy journal

MDPI

Article

A Spectroscopy-Based Multi-Analytical Approach for Studies in Conservation: Decorations in the Alexander Palace (Tsarskoye Selo)

Marilena Ricci [1], Federico Sebastiani [1], Maurizio Becucci [1,2,*], Mikhail Rogozny [3] and Vadim Parfenov [4]

[1] Department of Chemistry 'Ugo Schiff', University of Florence, Sesto Fiorentino, 50019 Florence, Italy
[2] European Laboratory for Non-Linear Spectroscopy, University of Florence, Sesto Fiorentino, 50019 Florence, Italy
[3] Department of Painting and Restoration, The St. Petersburg Stieglitz State Academy of Art and Design, 191028 St. Petersburg, Russia
[4] Department of Photonics, St. Petersburg Electrotechnical University, 197376 St. Petersburg, Russia
* Correspondence: maurizio.becucci@unifi.it

Abstract: We studied the painted decorations found during recent restoration work in the Alexander Palace in Tsarskoye Selo. Optical/laser spectroscopic methods were applied to obtain a characterization of the materials, pigments, and binders in use and, possibly, their degradation. We analyzed samples of the original Art Nouveau style decoration that was detached in 2019 during conservation work at the State Office of Emperor Nicholas II. A combination of Raman microscopy, infrared spectroscopy, and elemental analysis (obtained from the optical emission following laser plasma formation) allowed us to obtain detailed information on the materials used. The precious pigments of the artist's green-blue palette and the binder used (drying oil) were identified. A mixture of blue (Prussian blue and ultramarine blue), white (lead white and barium white), and yellow (chrome yellow and zinc yellow) pigments determined the different blue hues used. The use of bronze paint in the dark blue area, which was identified as a brass powder applied with a drying oil as a binder, was also demonstrated.

Keywords: cultural heritage; laser diagnostics; conservation of mural painting; pigments

Citation: Ricci, M.; Sebastiani, F.; Becucci, M.; Rogozny, M.; Parfenov, V. A Spectroscopy-Based Multi-Analytical Approach for Studies in Conservation: Decorations in the Alexander Palace (Tsarskoye Selo). *Spectrosc. J.* **2023**, *1*, 121–136. https://doi.org/10.3390/spectroscj1030011

Academic Editor: Clemens Burda

Received: 4 July 2023
Revised: 24 August 2023
Accepted: 2 October 2023
Published: 20 October 2023

1. Introduction

Characterizing real samples from a country's cultural heritage poses many questions for restorers and conservation scientists, and clear answers from a single (possibly simple and low-cost) analytical method cannot be obtained. The complexity present in samples arises from the possible superimposition of materials from the original manufacture and from later (and often not well-documented) restorations. The materials in use can be simple inorganics or mixtures of organic molecules extracted from plants or animals. Therefore, it is advisable to develop procedures aimed at the integration of different experimental methods that can provide complementary information at a reasonable cost and eventually be directly used in the field.

The integration of optical spectroscopic methods represents a possible solution to this problem, as they can provide complementary information on the atomic and molecular composition of the materials present in small areas (micrometers to millimeters in size) of the artwork without the stringent requirement of macroscopic sampling and sample destruction.

Many examples of this kind of multi-analytical spectroscopic approach have been reported [1–12] and integrated instruments have been proposed [1,13–15].

Herein, we report on the application of combined Raman and infrared vibrational spectroscopies with laser-induced breakdown atomic spectroscopy for the characterization

of the materials, pigments, and binders in use in the historical Alexander Palace (Russia). Preliminary results have already been reported in a previous publication [16].

In brief, micro-Raman spectroscopy is currently considered an established technique for material analysis and is widely accepted as a powerful analytical tool for art conservation and archaeological science, mostly concerning pigment identification [17,18]. It offers high sensitivity and specificity, enabling a non-invasive analysis of a wide variety of inorganic and organic materials with a very high spatial resolution. Nevertheless, the presence of organic molecules possibly fluorescing under laser excitation may limit the effectiveness of Raman spectroscopy, as the strong fluorescence in the background could mask the weak Raman bands. It represents a convenient extension of the more traditional infrared spectroscopic methods; however, vibrational spectroscopies are not always very informative regarding the presence of inorganic materials. Therefore, a combination of molecular and elemental information seems to be crucial for a complete and reliable qualitative (and quantitative) study. In regard to elemental analysis techniques, laser-induced breakdown spectroscopy (LIBS) provides information about the chemical composition of materials. LIBS offers a rapid and sensitive method for in-depth characterization that can be performed on site without sample preparation [19,20]. In favorable cases, LIBS allows the identification and quantification of even light elements, such as C, H, N, and O. The statistical elaboration of combined data produced via different experiments could make the overall data analysis process more robust.

When working with combined spectroscopic methods, another relevant issue is the possibility of carrying out different measurements in the same area of a sample with a spatial resolution in the order of 1 μm. This represents a significant advantage in the case of micro-structured samples, as it greatly increases the possibility of obtaining information on sample areas with a simple and well-defined chemical composition. Only a few laboratory-grade instruments offer this possibility, and in many cases, the sampling points and investigated volume are different when using different methods. The most commonly available instrumentation does not allow different measurements to be carried out at the same point, without sample displacement. In a case like this, data analysis is more complex, and the degree of confidence in the identification of the different components is lower.

The Alexander Palace was the favorite residence of Nicholas II, the last Russian Emperor, and it was connected to many events in his life. It was his place of birth and he was imprisoned there under house arrest with his family in March 1917, before being sent into exile in Tobolsk. The Italian architect Giacomo Quarenghi was commissioned by Catherine II to build the Alexander Palace in Tsarskoye Selo for her grandson, the future Emperor Alexander I, and it was built in 1792–1796. The original interior decoration, also by Quarenghi, was designed in the style of classicism. Unfortunately, almost nothing has been preserved from the initial interior decoration. The owners of the palace repeatedly changed; at different times, Nicholas I lived there, and both Alexander II and Alexander III spent their youth in the palace. The interior design changed depending on the tastes and preferences of the owners. Large alterations to the palace were completed during the reign of the last Emperor, Nicholas II. Personal apartments were rebuilt in the Art Nouveau style, which was fashionable at that time. The Nicholas II State Office was created by the architect R. Meltzer in 1902–1904. The office was connected with a mezzanine to the living room of his wife, Alexandra Feodorovna.

After the palace was nationalized in 1918, a museum was opened in the ceremonial halls and personal chambers of the last Emperor and Empress until 1941. The head of the museum, V. I. Yakovlev, wrote, describing the office: "The ceiling was lined with mahogany, the walls were painted with mastic oil paint of blue-green color and painted with a stencil with ornamental friezes around the tiled cladding over the fireplace and the niche behind the desk" [21].

During World War II, Tsarskoye Selo was occupied by the invading army and the Alexander Palace became the headquarters of the Spanish Blue Division and the Gestapo

branch in the basement of the prison [22]. The palace was badly damaged during the war. The first post-war restoration work was carried out during 1946–1951 in a project led by the architect L. M. Bezverkhny. The general concept for this project was the restoration of the interiors in the general style of the palace for the period of Quarenghi [23]. The remnants of the destroyed interiors, not corresponding to the general style of the building, were dismantled. During this period, the picturesque decoration of the State Office was also destroyed.

More recently, during the 2019 restoration, on two walls of the office, under the recent stucco, fragments of old pictorial decoration were found depicting, in the Art Nouveau style, a repeating ornament of stylized bunches of needles and pine cones. The paint layer was stratified and partially detached. In addition, it showed differences in color and tone in different areas. Therefore, restorers and museum staff of the Tsarskoe Selo State Museum and Heritage Site need to identify the original materials in order to plan the restoration of the historical mural paintings.

Herein, we report the characterization of small samples detached from the two walls during the conservation work to gain information on the pigments and binders used in the cabinet (and, possibly, on their degradation). We concentrated on comparison of the composition of various layers obtained by LIBS, and focused on the distribution of some specific elements (like Zn, Fe, Pb, Cu, and Sn) in an attempt to classify the paintings according to their content. These measurements were complemented by the characterization of materials at a molecular level by means of vibrational spectroscopic methods (IR and Raman).

2. Materials and Methods

2.1. The Painting and Its Conservation

The painting was in disrepair; the plaster layer was deformed along the edges of the chips, the paint layer was stratified and persistent, and stubborn dirt was present over the entire surface. Fragments of the painting located on opposite walls differed in color and tone.

Macroscopic observation of the samples suggested that the surface preparation for painting was carried out according to the system of putties and primers, with intermediate gluings by impregnation with drying oil. The putty layer has a thick leveling, beige color, apparently with a high content of gypsum. The paint layer seems to have been realized using the mastic-oil painting technique (which usually includes the use of pigments, wax, drying oil, and turpentine). The paint layer (background) is blue-green, dense, applied in several layers, while the lower layers are lighter. To achieve a uniform surface, the last layer of the background was applied by brushing (this method was common in the late XIX and early XX centuries). The ornament was stenciled, followed by writing with brushes. The texture of the brushstrokes is clearly visible on the pine needle images; the paint was applied thickly, with strokes in the direction of the drawing, and the edges are sharp. A characteristic bronze paint was used for some elements of the painting (Figure 1), typically consisting of a very fine metal powder mixed with oil varnish.

Figure 1. Decorations located on opposite walls of the State Office of Emperor Nicholas II in the Alexander Palace in Tsarskoye Selo. The points from which the samples analyzed in the laboratory were taken are marked in red and numbered. The sampling point number is used along the text to name the samples, i.e. sample 1 was taken from the sampling point number 1.

2.2. Experimental Methods

The experimental LIBS setup has been described previously [1,2]. Plasma was generated on the sample surface by laser pulses at 532 nm (approx. 2–5 mJ) from a Q-switched Nd-YAG laser (Big Sky Lasers, Bozeman MT, USA; model CFR 200-GRM, 8 ns pulse duration, 20 Hz, and top hat profile of constant energy density). The emission spectrum was acquired using a single grating spectrometer (Acton Research, Acton, MA, USA; model Sp2358i, 320 mm focal length, equipped with a holographic grating (150 lines/mm, blazed at 500 nm)), and an intensified CCD camera (Princeton Instruments, Trenton, NJ, USA; model PI Max-1024/RB-PTG, gated starting at 100 ns after laser Q-switching, 1 ms exposure). A small time delay after laser emission helps to avoid detection of the laser pulse itself and to strongly reduce the continuous background signal caused by electron relaxation in the plasma, the so-called *Bremsstrahlung* process. The reported spectra were obtained by averaging the emission following three consecutive laser pulses applied at the same point of the sample. Measurements were carried out at 3–5 random points in the different representative areas of the samples. The monochromator grating was set to a 450 nm central frequency, and a single data acquisition session of the 260–640 nm spectral region was investigated. The spectral resolution was approximately 1 nm along the spectrum. If needed, the spectra were smoothed by applying the Savitzky–Golay algorithm (second-order polynomial function applied on a 5-point window). The plasma was formed on a 30 μm-diameter spot. In some cases, a depth profile of the sample was obtained by repeating the data acquisition session in the same area of the sample 3–5 times without any adjustment in the optical system [2,24]. From the optical microscopy measurements, we estimated a penetration depth of approx. 20 μm per data acquisition session (3 laser pulses) [1,2].

The LIBS spectra were analyzed using both the sets of atomic transitions calculated from the LIBS data bank [25] (which is freely accessible on the NIST web site: https://physics.nist.gov/PhysRefData/ASD/LIBS/libs-form.html; last accessed on 24 August 2023) and a calibration-free method [26]. The atomic emission spectra were calculated on the hypothesis of a local thermodynamic equilibrium in the plasma and assuming an optically thin system (i.e., neglecting possible self-absorption phenomena, more likely for the stronger lines) [27]. The plasma equilibrium temperature was set to 0.6 eV (approximately 7000 K) after some initial tests. The calculated transitions were spectrally broadened with a Gaussian function (1 nm FWHM) in order to match the experimental conditions. We numerically adjusted the weight of the different atomic emission sets to match the spectral intensity distribution experimentally observed and to infer the different relative

atomic abundances in the samples. The error in the relative intensities can be quite large as the line intensities are strongly affected by both the plasma temperature and the effective quantitative transfer of the sample constituents into the plasma by laser excitation. The presence of the reported atomic species is clearly evident from the analysis. In fact, we noted only atomic species whose presence is univocally determined by the appearance of characteristic sets of atomic lines with appropriate relative intensities.

Raman spectra were obtained by using a Renishaw (Wotton-under-Edge, UK) RM2000 Raman microscope, which consists of a single grating monochromator (1200 lines/mm, with an approximately 4 cm^{-1} spectral resolution) with a cooled CCD detector optically coupled to a Leica optical microscope. Notch filters were employed to decouple the Rayleigh and Raman scattering. The laser beam was focused on the sample using microscope objectives up to 100×, allowing for a better than 1 μm spatial resolution. Both 514 and 785 nm laser radiations, from an argon ion laser and a diode laser, respectively, were used. The laser power on the sample was adjusted between 0.01 and 2 mW. The typical integration time for the acquisition of a Raman spectrum was between 10 and 100 s. In some cases, fragments were prepared for Raman stratigraphic analysis by casting them in a polymer and optically cleaning the surface.

Plasters and pigments were investigated by Fourier transform infrared (FTIR) spectroscopy in attenuated total reflectance mode (by placing the samples on a diamond crystal) using a Spectrum 100 Perkin Elmer (Waltham, MA, USA) with an attenuated total reflectance (ATR) attachment. The detector is based on a fast recovery deuterated alanine-doped triglycine sulfate sensor and works in a spectral range of 4000–380 cm^{-1} with a spectral resolution of 4 cm^{-1}. The instrument collects data from a macroscopic area, with a 5 mm diameter.

3. Results and Discussion

Figure 2 shows, both as a cross-section and front view, a typical sample in the blue area with its complex stratigraphic distribution of the different materials. In all cross-sections of the samples, it is possible to recognize four layers of different thicknesses on top of the ground preparatory layer. From bottom to top (indicated by the vertical arrow), two layers consist of two shades of white paints, one of a light brownish color, and another slightly clearer. Above, a light blue layer is visible that is superimposed on a thick blue layer, where grains of blue pigments are coarsely mixed with dark paint. In addition, a front view of the sample shows the holes produced during the LIBS experiments after prolonged laser exposure.

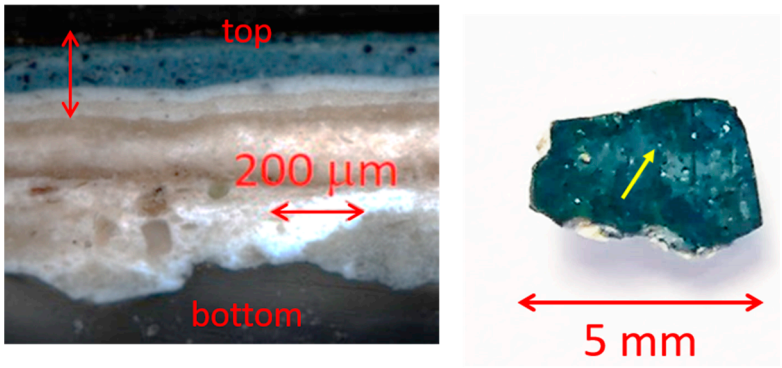

Figure 2. Stratigraphic section and front view of a typical blue sample (sample 2). The vertical arrow in the cross-section indicates the four painting layers described in the text. The cross-section prepared for Raman stratigraphic characterization was taken from the right side of the sample. The arrow indicates the local damage (less than 0.1 mm in diameter) made by the laser ablation process after multiple laser shots.

The most intense bands in the experimental spectrum (e.g., Cu bands at 324 and 327 nm and Ca bands at 393, 397, and 420 nm) are possibly attenuated by self-absorption in the plasma. This phenomenon is easily recognized by large discrepancies between the intensity ratios of the bands assigned to the same atomic species. Therefore, we prefer to use only the weak bands to evaluate the relative abundancies of the different atomic species. Furthermore, LIBS experiments have a very limited sensibility for many atoms (e.g., light atoms from the first and second periods, halogens, and chalcogens) due to their small cross-sections in the VIS-UV spectral range. In addition, the extraction of quantitative information is hindered by the large differences in the relative cross-sections for the emission lines of different elements. Therefore, in the following discussion, we limited the presentation of the results to the statement of the presence (or large presence) of given elements. Finally, the possibility of quantitative analysis is limited by the inhomogeneity of these samples and the large number of constituent materials (which lead to overlapping of many atomic lines in the experimental spectra). Despite all of the limitations discussed above, when working on samples containing bronze paint, we made a particularly strenuous effort to obtain a more accurate determination of its chemical composition. We took as a standard a known metal alloy (Nordic gold, the alloy used for 10, 20, and 50 Euro cent coins, which contains 89% Cu, 5% Zn, 5% Al, and 1% Sn). An example of the experimental LIBS atomic emission spectrum obtained in the bronze paint area, together with its numerical simulation, is reported in Figure 3 (left panel). The LIBS measurements on the different samples of the painting show the presence of multiple elements. Indeed, the dimension of the laser spot was approximately 30 μm, larger than the typical dimension of the grains and comparable with the layer thickness (as shown in Figure 2). The LIBS measurements carried out in the area covered with bronze paint showed the strong, characteristic bands of Cu (324.7 and 327.4 nm). By repeating the measurements in the same spot, we observed a drastic reduction of the signal after the first laser shot, indicating that only a thin layer (<20 μm) of this pigment is present on the surface. Very close to the strong Cu lines, the weak peak of Zn (334.5 nm) was observed in these samples. The characteristic atomic emission lines of Sn (284.0 and 317.5 nm) were not detected in the spectrum (see, in Figure 3, the comparison of the LIBS spectrum measured on the bronze paint (left side) with that measured on the Nordic gold alloy (right side)). An analysis of the relative intensities of the Zn and Cu lines indicates the use in a bronze paint based on a copper-based alloy containing a 3–5% abundancy of zinc.

The LIBS spectra, taken at spots on the blue and light blue paint (Figure 4, left and right), display the main emission features characteristic of Ca, Ba, Fe, Al, Na, and Pb, in different percentages in addition to several elements of lower concentrations, and thus suggest the presence of mixtures of pigments. Calcium was the most abundant element in all of the blue paint areas we investigated, suggesting that calcium carbonate or gypsum were used as a white pigment. Likewise, barium and zinc lines were also evident in the LIBS spectra, which can be attributed to either the use of barium sulfate and zinc oxide or lithophone (a mixture of barium sulfate and zinc sulfide), used either as a matrix material or as an extender in the paint.

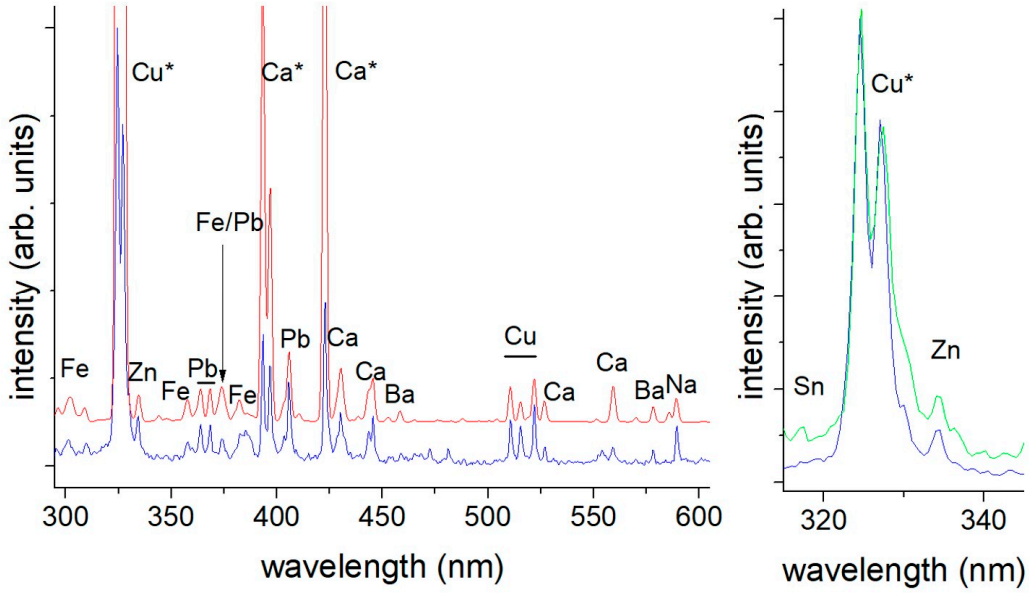

Figure 3. LIBS spectrum measured in the bronze-painted area (sample 3) with its numerical simulation (left panel—bottom, blue trace are experimental data and upshifted red trace is a numerical simulation). The major peaks are labeled with the associated atomic species. A few strong peaks (*) have different intensities in the experimental and simulated spectra due to self-absorption in the plasma. Right panel, experimental LIBS data measured on the bronze paint (bottom, blue line) and on the Nordic gold metal alloy (upshifted, green line) compared in the spectral region of the Sn, Cu, and Zn lines.

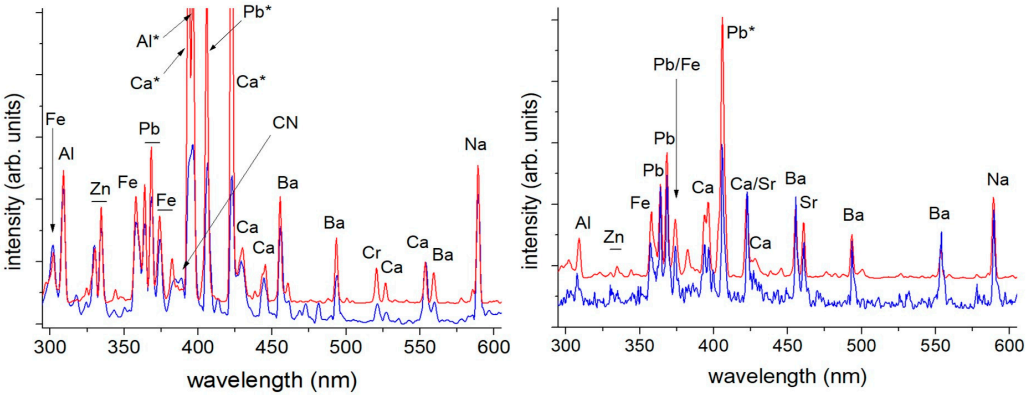

Figure 4. LIBS spectra measured at different points of the blue area of sample 4 with their numerical simulations (blue traces are experimental data and upshifted red traces are numerical simulations). The major peaks are labeled with the associated atomic species. A few strong peaks (*) have different intensities in the experimental and simulated spectra due to self-absorption in the plasma. The possible presence of the CN signal at 388 nm is marked (left spectrum).

The origin of the Pb emission line, possibly associated either with lead oxides (Pb_3O_4, PbO, and PbO_2) or lead carbonates ($Pb(OH)_2{\cdot}2PbCO_3$ and $PbCO_3$), requires further investigation by other molecular analysis techniques. The presence of iron lines could be related to an iron-based pigment; in such a case, the color of the paint is important for identifying the pigment present, tentatively assigned as Prussian blue. The combined presence of the intense Na and Al lines in the LIBS spectrum on the blue surface (Figure 4) and their reduced contribution after a few laser shots provides good evidence for confirming the identity of the ultramarine pigment. In addition, the LIBS spectrum in the darker blue area (Figure 4, left) was also characterized by molecular emission at 386 nm from the excited CN radical, usually related to the presence of a material containing sp^2 carbon and possibly

originating from the presence of an organic binder or the use of carbon black. Indeed, the presence of chromium at a low concentration in the first layer of the blue areas could be ascribed to chromium green (Cr_2O_3) or to chromium yellow (a pigment containing lead chromate; $PbCrO_4$).

Therefore, to gain greater insight into the composition and identity of the different pigments used in multi-component mixtures and/ or in different paint layers, microRaman spectra were acquired on both the cross-sections and the surfaces of the samples. The two white primer layers below the blueish layers, one bright and the other slightly light brown (Figure 2), are distinguished by different mixtures of pigments. In the lighter and bright layer is lead white with barium sulfate and little calcite, while in the (light brown) darker one, there is calcite and/or gypsum with a small amount of white lead (Figure 5). Barium sulfate, known as barium white and found as the mineral barite, was already indicated as an artist's pigment in 1782–1783. However, it became widely used only at the beginning of the XIX century, both in its natural and synthetic forms, mostly as an extender to lead white [28]. It is well known that over time, the method of preparation of painting substrates changed and artists used different types of primers. Therefore, the composition and structure of the ground layer(s) in some cases can represent a possible indicator of when the artwork was painted. Therefore, the results of this study can provide important information for dating and attributing works by artists of this period [25].

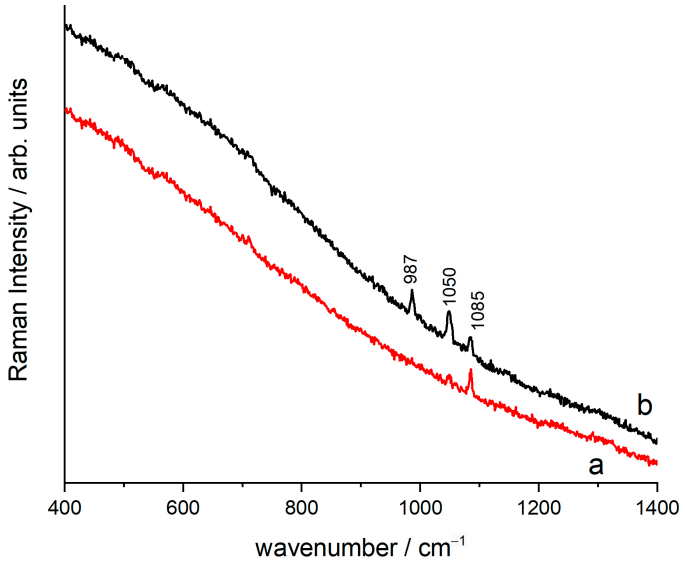

Figure 5. Raman spectra of the two white primer layers in sample 2. Bands derived from lead white (1050 cm^{-1}), barium sulfate (987 cm^{-1}), and calcite (1085 cm^{-1}) in different mixtures can be observed. Trace (**a**) is measured on the light brown layer, while trace (**b**) on the white bright layer.

The LIBS results show the presence of Zn in the blue and white upper layers, supporting the hypothesis of the use of zinc oxide or lithopone as pigments. We did not observe the characteristic band of ZnS at 348 cm^{-1} in the Raman spectra, while the sulfate band at 987 cm^{-1} is clearly observed; therefore, the presence of lithopone is unlikely. Conversely, as zinc white is a not an efficient Raman scatterer and because it was mixed with other pigments that give rise to more intense bands in the relevant spectral range, it could not be identified by micro-Raman spectroscopy. The fact that zinc was identified both on the paint layer and the first primer layer suggests that zinc white was probably used by manufacturers to lighten the hues of other pigments and as extender. Zinc white, in a mixture with chalk and lead white as primers, has been previously identified in modern Russian paintings [29].

The micro-Raman spectroscopy complemented the LIBS data and demonstrates that both Prussian blue and ultramarine blue were used. Prussian blue ($Fe_4[Fe(CN)_6]_3$) is

an iron(III) hexacyanoferrate(II) complex, whose color is determined by an intervalent charge transfer between iron(II) and iron(III) ions mediated by the cyano group. The ν(CN) vibrations between 2070 and 2160 cm^{-1} are the spectral signature of this pigment. The C≡N group shows Raman active bands at different wavenumbers in this range, as it is coordinated with iron ions of different valence states. The main peak around 2155–2160 cm^{-1} is assigned to the A_{1g} ν(CN) stretching vibration bridging with iron(II) and iron(III) atoms, showing a shoulder toward lower wavenumbers at 2123 cm^{-1}, typically associated with the presence of CN^- ions. The other peak, at 2090 cm^{-1}, is assigned to the E_g mode of the ν(CN) stretching vibration [30]. Other characteristic peaks are located in the lower end of the spectrum, in the range between 190–340 cm^{-1} and 450–620 cm^{22121}. The first spectral window (190–340 cm^{-1}) shows a major peak at 276 cm^{-1} assigned to vibrations of the Fe–CN–Fe bond [30] (see Figure 6). In the second spectral window (450–620 cm^{-1}), a major peak at 537 cm^{-1} and a shoulder at 605 cm^{-1} are present, characteristic of all Fe–C lattice stretching vibrations.

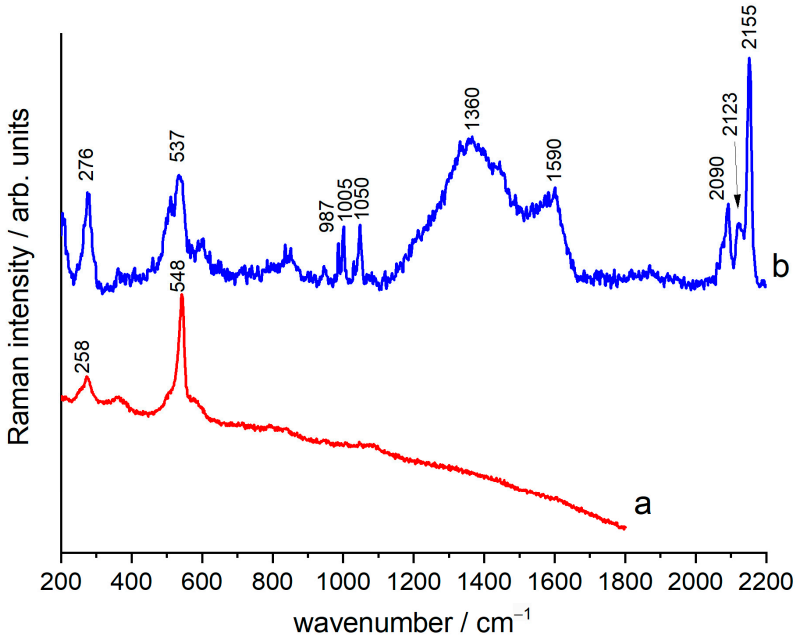

Figure 6. Raman spectra measured in blue areas of the sample. Bands characteristic of ultramarine blue (trace (**a**), sample 2) and Prussian blue (trace (**b**), sample 1) clearly identify the pigments present in each sample. The other vibrational bands are due to amorphous carbon (1360, 1590 cm^{-1}) lead white (1050 cm^{-1}), barium sulfate (987 cm^{-1}), and gypsum (1005 cm^{-1}).

The characteristic bands of ultramarine (a pigment originally made of grinded natural lapis lazuli and available as a synthetic material since ~1830) are located near 548 cm^{-1} (ν_1 (A_1), assigned to the totally symmetric stretching vibration of S_3^- ions) and 258 cm^{-1} (ν_2 (A_1), bending vibration of S_3^- ions), with a shoulder near 585 cm^{-1} (assigned to the stretching vibration of S_2^- ions) [31].

Different hues of blue are obtained by changing the quantity of blue pigments and adding different amounts of white pigments/extenders that also influence their working properties. In the dark blue areas, there is more Prussian blue and sometimes amorphous carbon. The tinting strength of Prussian blue is so high that it is rarely used undiluted; a relatively large amount of extender could be added by the pigment manufacturer or painter to improve the properties of the material for decorative applications without greatly reducing the strength of the color.

The greenish nuances in the painting were obtained using different mixtures of pigments. In the first layer of sample 1, the micro-Raman spectra revealed the presence of different pigments, including ultramarine, lead white, and barium sulfate. The green

pigment was identified as chrome green, a mixture of Prussian blue and chrome yellow. Chrome green is produced as a mixture of the constituent pigments finely grinded, resulting in a powder with a very small particle size. Therefore, the grains of the individual constituents could not be individually identified in micro-Raman experiments using low magnification objectives and the mixture appeared to be a single pigment. However, its Raman spectrum (Figure 7a) displays bands typical of both chrome yellow (842, 360 cm^{-1}) and Prussian blue (2152, 2090, 276 cm^{-1}). Instead, in the bright blue greenish area observed in other samples, a different yellow pigment was used, together with blue pigments, to obtain the green color (Figure 7b).

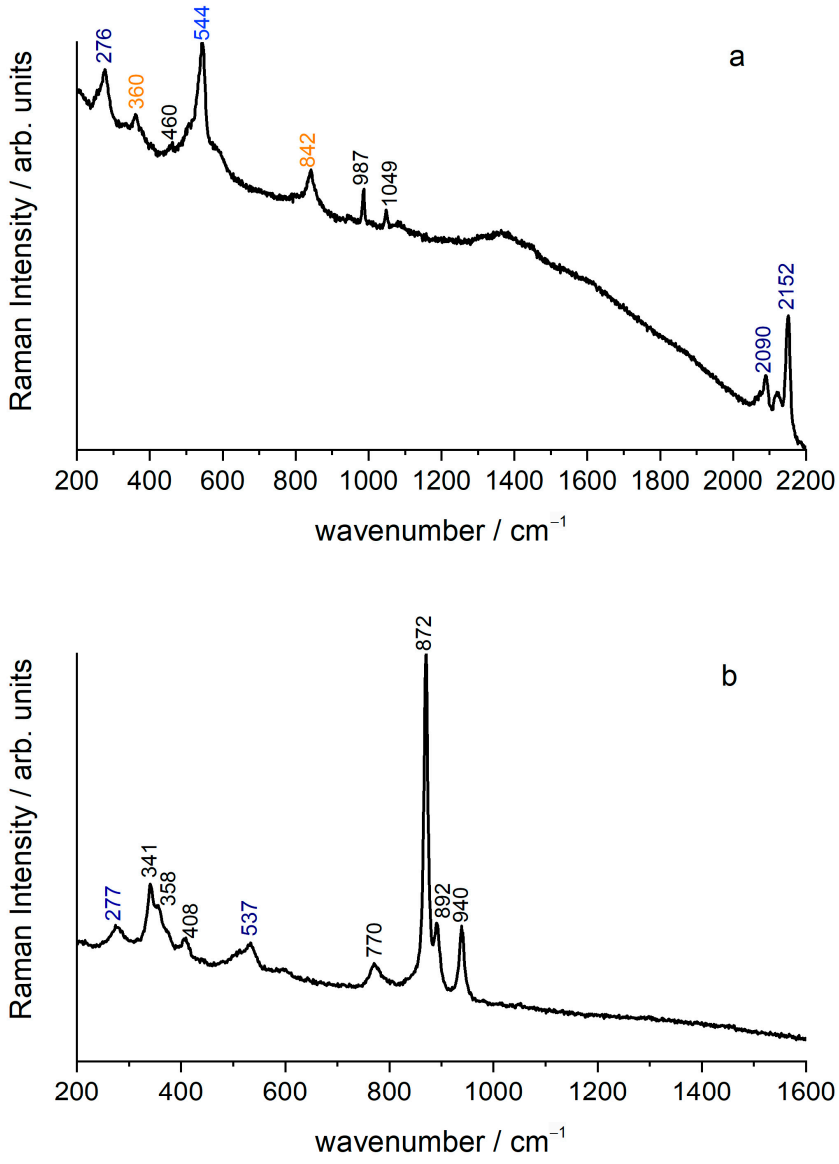

Figure 7. (**a**) Raman spectrum of the first layer in sample 1, where bands ascribed to Prussian blue (dark blue), ultramarine (blue), and chrome yellow (orange) can be observed. The other vibrational bands are due to barium sulfate and lead white. (**b**) Raman spectrum of the area of greenish color in sample 5, displaying mainly bands assignable to zinc potassium chromate hydrate (black) and Prussian blue (blue).

The zinc potassium chromate hydrate (K_2O $4ZnCrO_4$ $3H_2O$) was identified by Raman bands at 341(m), 358(m), 376(w), 408(m), 770(m), 872(vs), 892(m), and 940(s) cm^{-1} (Figure 7b). It was also found in the orange-gold part of the paintings. By comparison with

the vibrational assignments of other chromates [32–34], the strong band at 872 cm^{-1} can be assigned to the CrO_4^{2-} symmetric stretching vibration ν_1, and the bands at 940, 892, and 770 cm^{-1} to the asymmetrical stretching mode ν_3. The bending modes ν_2 and ν_4 are located at 408, 376, 358, and 341 cm^{-1}.

Zinc potassium chromate is not a commonly used pigment; however, it has been identified in some of Munch's paintings ("Sick Child" (1885–1886), "Scream" (1893), and "Melancholy" (1894) [35]), which are almost contemporary with the Alexander Palace's decorations. In terms of combinations of pigments, the presence of Cr and Zn in bluish/green shadows could also be explained as being due to the presence of chromium oxide green and zinc white. The micro-Raman spectroscopy disproved this possibility, showing that both blue (Prussian blue and ultramarine) and yellow pigments are present.

The LIBS data show that the bronze paint was made using a copper-based alloy. The microscopic images demonstrate that it was applied as a powder with a ligand (not as a decoration made with a metal foil). The Raman spectra measured in these areas show the oxidation products of copper, such as cuprite and tenorite (Figure 8), in the different regions analyzed. In the black area, tenorite is present, whose spectrum is dominated by a band at 290 cm^{-1}, together with weak bands at 335 and 620 cm^{-1} [36,37]. The Raman spectrum collected from the golden area of sample 3 shows a strong peak at 218 cm^{-1}, possibly ascribed to the characteristic vibrational mode of cuprite, and weak, broad bands at 418, 515, and 625 cm^{-1}. These weak bands can be assigned to amorphous Cu_2O [38], which are characteristic of defective cuprite that forms native passive layers on copper or bronze objects.

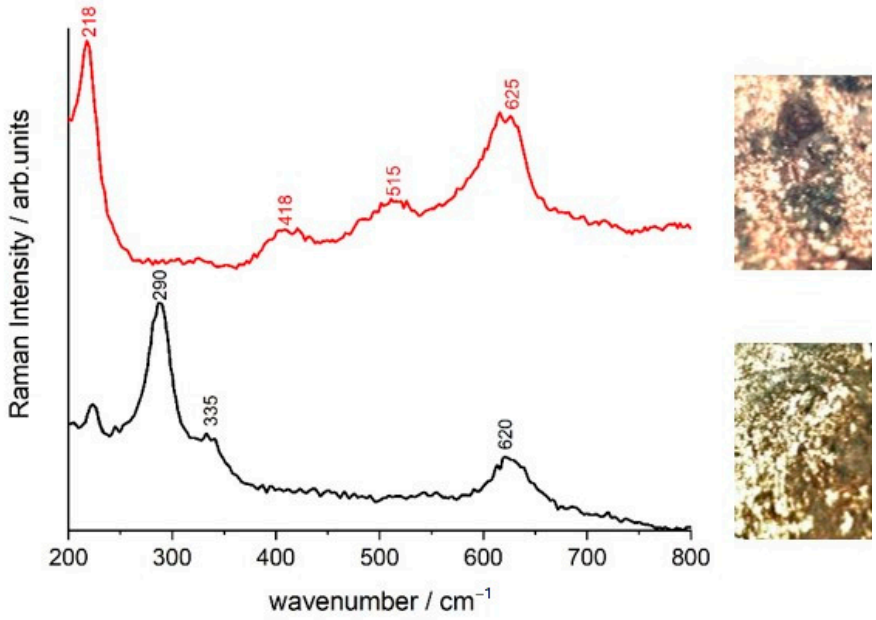

Figure 8. Raman spectra measured at different points of the bronze paint, showing the presence of cuprite (top trace, sample 3) and tenorite (bottom trace, sample 1).

The reported results provide a clear demonstration that micro-Raman spectroscopy is a powerful tool for the identification of pigments, which cannot be unambiguously differentiated by LIBS. However, micro-Raman spectroscopy commonly does not detect all materials present in a sample and should be combined with additional analytical methods to assure a reliable and complete pigment characterization.

All samples were also analyzed by ATR-FTIR spectroscopy. In addition to the presence of pigments that characterize blue and white colors, bands are visible that could be associated with the presence of a binder or protective. Assignment of the major bands to different chemical components or specific vibrations provides insight to better identify the material

that gives rise to these bands. In fact, stretching vibrations of the C=O group of esters and carboxylic acids, at 1732 and 1705 cm^{-1}, respectively, and the asymmetric and symmetric CH_2 stretching vibrations at 2920 (ν_{AS}-CH_2) and 2851 (ν_{SY}-CH_2) cm^{-1}, respectively, indicate the presence of a drying oil as the binding medium used. The sharp bands at 1586 and 1546 cm^{-1} with a double peak at 1536 cm^{-1}, shown in Figure 9, are attributed to metal carboxylates, which are the result of a saponification process between drying oil, mainly composed of triglycerides (i.e., esters of glycerol linked to three long-chain carboxylic acids) and metal-based pigments [39].

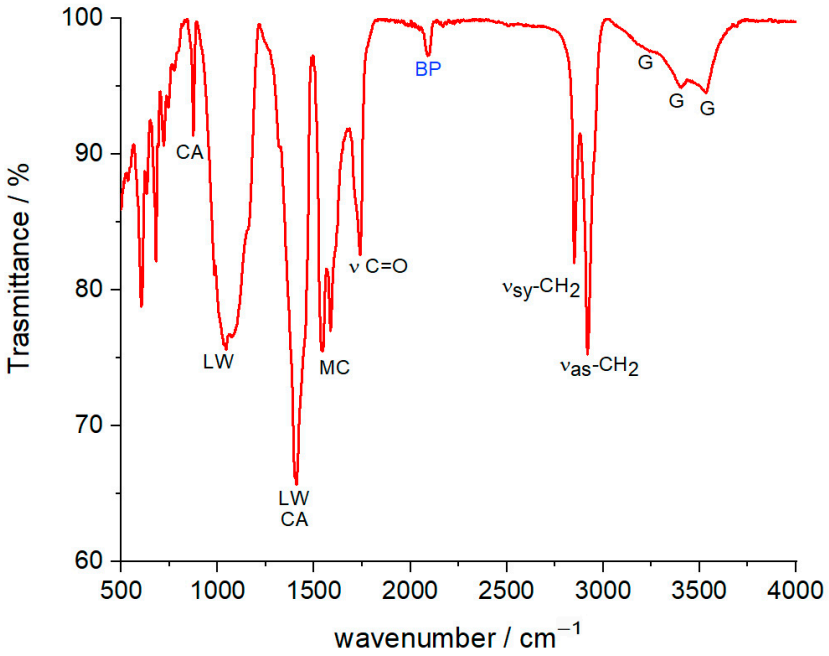

Figure 9. ATR-FTIR spectrum of sample 1 with assignment of the major bands to different chemical components or specific vibrations: BP, Prussian blue (2089 cm^{-1}); MC, metal carboxylates (1586, 1546, and 1538 cm^{-1}); G, gypsum (3542 and 3398 cm^{-1}); LW, lead white (1398 and 1045 cm^{-1}); CA, calcite (1400 and 875 cm^{-1}).

Drying of the oil predominantly results from photo-oxidation and autoxidation reactions. The double bonds of the unsaturated fatty acids are quite reactive and are primarily involved in these reactions that might be catalyzed by the metal ions originating from pigments and/or driers. This chemical process results in the formation of a complex three-dimensional polyanionic network based on the glycerol ester, with crosslinking provided by a fraction of carboxylate anions stabilized by metal cations. A fraction of mono- and dicarboxylic acids that is not incorporated into the polyanionic network may migrate to react with metal cations, leading to the formation of metal carboxylates (metal soaps). The formation of metal soaps can be clearly identified in infrared spectroscopy as a result of the characteristic bands associated with the COO group's asymmetric stretching vibration for copper (1586 cm^{-1}), lead (1546 cm^{-1}), and zinc (1546 and 1538 cm^{-1}) carboxylates. The identification of metal soaps in the FTIR spectra measured on the painting samples confirms the use of drying oil as a binder.

Finally, the spectra show the presence of gypsum (calcium sulfate hydrate, $CaSO_4 \cdot 2H_2O$, with characteristic bands at 3522, 3396, 1620, 1111, and 668 cm^{-1}), suggesting its use as both a component of the preparation layer and/or as a common degradation product of calcite in wall paintings.

In regard to the state of conservation of the pigments, a chromatic alteration of the pictorial layer, mostly darkening, was visible in some areas. Nonetheless, there is no evidence from the Raman or FTIR spectroscopy that degradation products of the original

pigments can be held responsible for this chromatic change. Indeed, we found evidence for degradation of the binders used, and this process might be the most likely reason for the observed chromatic change. Furthermore, in the areas where the use of bronze paint was identified, an appreciable quantity of dark copper oxidative products was detected at a microscopic level.

In summary, study of the blue decorations of the State Office of Emperor Nicholas II has provided the first information about the palette in use, which includes several pigments, such as ultramarine, carbon black, lead white, zinc oxide, barium sulfate, Prussian blue, pure or blended with chrome yellow for light green hues, and zinc potassium chromate (zinc yellow). The mixture of blue, white, and yellow pigments determines the different greenish-blue hues. The use of a bronze paint identified as a brass powder applied with a drying oil as a binder was also shown. Raman analysis of cross-section samples demonstrated the use of different white pigments, such as lead white, chalk, gypsum, and barium white, in various compositions, giving rise to white and light brown ground layers. The results described above regarding the materials available to the artists at the time suggest that, generally, the palette and primers of modern artists in Russia and Europe were very similar. Indeed, modern Russian artists, like their predecessors, generally used paint materials imported from Europe, since, until the 1930s, only a few small factories in Russia produced paints. The binder in use was identified as a drying oil.

As a final remark, we wish to point out that in this kind of modern mural paintings, the use of organic dyes cannot be discounted. We did not find evidence for the use of these materials in the Alexander Palace. However, as these organic materials are often used in very limited amounts, quite often, vibrational spectroscopies do not provide high enough sensitivity for their identification. Therefore, alternative approaches based on different methods should be implemented in the case of further research in this direction. The use of electronic spectroscopic methods, such as fluorescence [40]/UV-vis reflectance [41], has shown good potential for this kind of application. Additionally, several authors have demonstrated that surface-enhanced Raman spectroscopy (SERS) is a very promising tool for the identification and quantification of organic dyes due to its remarkable sensitivity (detection of up to single molecule) together with the rich vibrational spectroscopic details that it can provide, despite its inherent experimental complexity [42–47].

4. Conclusions

We obtained new, complementary information on the materials and methods used for the Art Nouveau decoration in the State Office of Emperor Nicholas II (the Alexander Palace in Tsarskoye Selo, Russia). This study was carried out by the combined use of different spectroscopic methods, an approach that is of quite general applicability and highly suitable for qualitative analysis of many different materials at the atomic and molecular levels. The correlation of data arising from different spectroscopic observables enabled us to provide a deeper understanding of the system.

On the basis of this work, it was possible to demonstrate that on one of the sections of the painting, there was a darkening, mostly associated with either the degradation of the binders used or the oxidation of the copper in the bronze paint. The use of chromates to produce different green-blue hues was also demonstrated. The Methodical Council of the Tsarskoe Selo State Museum and Heritage Site have exploited these results to implement a plan of conservation and restoration of the State Office and to choose an appropriate palette of colors and pigments. Fragments of the original painting are conserved in the museum as reference materials and available for further studies.

Author Contributions: Conceptualization, M.R. (Mikhail Rogozny), V.P., M.R. (Marilena Ricci) and M.B.; methodology, M.R. (Mikhail Rogozny), V.P., M.R. (Marilena Ricci) and M.B.; validation, M.B. and M.R. (Marilena Ricci); formal analysis, F.S.; investigation, V.P., M.R. (Marilena Ricci), M.B. and F.S.; resources, M.B.; data curation, M.B., M.R. (Marilena Ricci) and F.S.; writing—original draft preparation, M.B. and M.R. (Marilena Ricci); writing—review and editing, M.R. (Mikhail Rogozny), V.P., M.B., M.R. (Marilena Ricci), and F.S.; visualization, M.R. (Marilena Ricci); supervision, M.R.

(Marilena Ricci), M.B. and V.P.; funding acquisition, M.B. and V.P. All authors have read and agreed to the published version of the manuscript.

Funding: A bilateral agreement between the University of Florence and LETI—Saint Petersburg to provide travel support to V.P.

Data Availability Statement: Data are available upon reasonable request to the authors.

Acknowledgments: The authors thank B. Howes for carefully reading the manuscript and offering many suggestions.

Conflicts of Interest: The authors declare no conflict of interest.

References

1. Osticioli, I.; Mendes, N.F.C.; Nevin, A.; Zoppi, A.; Lofrumento, C.; Becucci, M.; Castellucci, E.M. A New Compact Instrument for Raman, Laser-Induced Breakdown, and Laser-Induced Fluorescence Spectroscopy of Works of Art and Their Constituent Materials. *Rev. Sci. Instrum.* **2009**, *80*, 076109. [CrossRef] [PubMed]
2. Mendes, N.F.C.; Osticioli, I.; Striova, J.; Sansonetti, A.; Becucci, M.; Castellucci, E. Versatile Pulsed Laser Setup for Depth Profiling Analysis of Multilayered Samples in the Field of Cultural Heritage. *J. Mol. Struct.* **2009**, *924–926*, 420–426. [CrossRef]
3. Burgio, L.; Clark, R.J.H.; Hark, R.R. Raman Microscopy and X-ray Fluorescence Analysis of Pigments on Medieval and Renaissance Italian Manuscript Cuttings. *Proc. Natl. Acad. Sci. USA* **2010**, *107*, 5726–5731. [CrossRef]
4. Bicchieri, M.; Ronconi, S.; Romano, F.P.; Pappalardo, L.; Corsi, M.; Cristoforetti, G.; Legnaioli, S.; Palleschi, V.; Salvetti, A.; Tognoni, E. Study of Foxing Stains on Paper by Chemical Methods, Infrared Spectroscopy, Micro-X-Ray Fluorescence Spectrometry and Laser Induced Breakdown Spectroscopy. *Spectrochim. Acta Part B At. Spectrosc.* **2002**, *57*, 1235–1249. [CrossRef]
5. Carlesi, S.; Ricci, M.; Cucci, C.; La Nasa, J.; Lofrumento, C.; Picollo, M.; Becucci, M. Multivariate Analysis of Combined Fourier Transform Near-Infrared (FT-NIR) and Raman Data Sets for Improved Discrimination of Drying Oils. *Appl. Spectrosc.* **2015**, *69*, 865–876. [CrossRef] [PubMed]
6. Vagnini, M.; Gabrieli, F.; Daveri, A.; Sali, D. Handheld New Technology Raman and Portable FT-IR Spectrometers as Complementary Tools for the in Situ Identification of Organic Materials in Modern Art. *Spectrochim. Acta Part A Mol. Biomol. Spectrosc.* **2017**, *176*, 174–182. [CrossRef] [PubMed]
7. Ghirardello, M.; Mosca, S.; Marti-Rujas, J.; Nardo, L.; Burnstock, A.; Nevin, A.; Bondani, M.; Toniolo, L.; Valentini, G.; Comelli, D. Time-Resolved Photoluminescence Microscopy Combined with X-Ray Analyses and Raman Spectroscopy Sheds Light on the Imperfect Synthesis of Historical Cadmium Pigments. *Anal Chem* **2018**, *90*, 10771–10779. [CrossRef]
8. Crupi, V.; Galli, G.; La Russa, M.F.; Longo, F.; Maisano, G.; Majolino, D.; Malagodi, M.; Pezzino, A.; Ricca, M.; Rossi, B.; et al. Multi-Technique Investigation of Roman Decorated Plasters from Villa Dei Quintili (Rome, Italy). *Appl. Surf. Sci.* **2015**, *349*, 924–930. [CrossRef]
9. Burgio, L.; Clark, R.J.H.; Stratoudaki, T.; Doulgeridis, M.; Anglos, D. Pigment Identification in Painted Artworks: A Dual Analytical Approach Employing Laser-Induced Breakdown Spectroscopy and Raman Microscopy. *Appl. Spectrosc.* **2000**, *54*, 463–469. [CrossRef]
10. Burgio, L.; Melessanaki, K.; Doulgeridis, M.; Clark, R.J.H.; Anglos, D. Pigment Identification in Paintings Employing Laser Induced Breakdown Spectroscopy and Raman Microscopy. *Spectrochim. Acta Part B At. Spectrosc.* **2001**, *56*, 905–913. [CrossRef]
11. Melessanaki, K.; Papadakis, V.; Balas, C.; Anglos, D. Laser Induced Breakdown Spectroscopy and Hyper-Spectral Imaging Analysis of Pigments on an Illuminated Manuscript. *Spectrochim. Acta Part B At. Spectrosc.* **2001**, *56*, 2337–2346. [CrossRef]
12. Chaplin, T.D.; Clark, R.J.H.; Martinón-Torres, M. A Combined Raman Microscopy, XRF and SEM–EDX Study of Three Valuable Objects—A Large Painted Leather Screen and Two Illuminated Title Pages in 17th Century Books of Ordinances of the Worshipful Company of Barbers, London. *J. Mol. Struct.* **2010**, *976*, 350–359. [CrossRef]
13. Zieba-Palus, J.; Borusiewicz, R.; Kunicki, M. PRAXIS—Combined μ-Raman and μ-XRF Spectrometers in the Examination of Forensic Samples. *Forensic Sci. Int.* **2008**, *175*, 1–10. [CrossRef] [PubMed]
14. Kansiz, M.; Prater, C.B. Super Resolution Correlative Far-Field Submicron Simultaneous IR and Raman Microscopy: A New Paradigm in Vibrational Spectroscopy. In *Advanced Chemical Microscopy for Life Science and Translational Medicine*; Simpson, G.J., Cheng, J.-X., Min, W., Eds.; SPIE: Bellingham, WA, USA, 2020; Volume 11252, p. 78.
15. Giakoumaki, A.; Osticioli, I.; Anglos, D. Spectroscopic Analysis Using a Hybrid LIBS-Raman System. *Appl. Phys. A Mater. Sci. Process.* **2006**, *83*, 537–541. [CrossRef]
16. Ricci, M.; Sebastiani, F.; Becucci, M.; Rogozny, M.; Parfenov, V. Study of the Picturesque Decoration of the State Office of Emperor Nicholas II in the Alexander Palace in Tsarskoye Selo. In *Optoelectronics into a Powerful Economy*; Rădvan, R., Ed.; AGIR Publishing House: Bucharest, Romania, 2020; pp. 337–346. ISBN 978-973-720-822-4.
17. Bersani, D.; Lottici, P.P. Raman Spectroscopy of Minerals and Mineral Pigments in Archaeometry. *J. Raman Spectrosc.* **2016**, *47*, 499–530. [CrossRef]
18. Bersani, D.; Conti, C.; Matousek, P.; Pozzi, F.; Vandenabeele, P. Methodological Evolutions of Raman Spectroscopy in Art and Archaeology. *Anal. Methods* **2016**, *8*, 8395–8409. [CrossRef]

19. Hahn, D.W.; Omenetto, N. Laser-Induced Breakdown Spectroscopy (LIBS), Part I: Review of Basic Diagnostics and Plasma-Particle Interactions: Still-Challenging Issues within the Analytical Plasma Community. *Appl. Spectrosc.* **2010**, *64*, 335A–336A. [CrossRef]
20. Hahn, D.W.; Omenetto, N. Laser-Induced Breakdown Spectroscopy (LIBS), Part II: Review of Instrumental and Methodological Approaches to Material Analysis and Applications to Different Fields. *Appl. Spectrosc.* **2012**, *66*, 347–419. [CrossRef]
21. Yakovlev, V.I. *Alexander Palace Museum in the Children's Village. Decoration*; Publication of the Administration of the Detskoselsky and Pavlovsk Palaces-Museums: Leningrad, Russia, 1928; p. 286.
22. Bardovskaya, L.V.; Plaude, V.F.; Stepanenko, I.G. *Alexander Palace. Album*; Aurora Publishing House: St. Petersburg, Russia, 2010; p. 42.
23. Bezverkhniy, L.M. Restoration of the Former Alexander Palace and Lyceum in the City of Pushkin. *Archit. Leningr.* **1950**, *1*, 23.
24. Kaszewska, E.A.; Sylwestrzak, M.; Marczak, J.; Skrzeczanowski, W.; Iwanicka, M.; Szmit-Naud, E.; Anglos, D.; Targowski, P. Depth-Resolved Multilayer Pigment Identification in Paintings: Combined Use of Laser-Induced Breakdown Spectroscopy (LIBS) and Optical Coherence Tomography (OCT). *Appl. Spectrosc.* **2013**, *67*, 960–972. [CrossRef]
25. Kramida, A.; Olsen, K.; Ralchenko, Y. NIST LIBS Database. Available online: https://physics.nist.gov/PhysRefData/ASD/LIBS/libs-form.html (accessed on 22 June 2023).
26. Tognoni, E.; Cristoforetti, G.; Legnaioli, S.; Palleschi, V. Calibration-Free Laser-Induced Breakdown Spectroscopy: State of the Art. *Spectrochim. Acta Part B At. Spectrosc.* **2010**, *65*, 1–14. [CrossRef]
27. Fantoni, R.; Caneve, L.; Colao, F.; Fornarini, L.; Lazic, V.; Spizzichino, V. Methodologies for Laboratory Laser Induced Breakdown Spectroscopy Semi-Quantitative and Quantitative Analysis-A Review. *Spectrochim. Acta Part B At. Spectrosc.* **2008**, *63*, 1097–1108. [CrossRef]
28. Feller, R.L. (Ed.) *Artists' Pigments. A Handbook of Their History and Caractheristics*; National Gallery, Washington and Cambridge University Press: Cambridge, MA, USA, 1986; Volume 1, p. 47.
29. Kadikova, I.; Pisareva, S. Primers of Modern Russian Artists: Composition, Structure and Dating. *Int. J. Conserv. Sci.* **2022**, *13*, 1485–1494.
30. Moretti, G.; Gervais, C. Raman Spectroscopy of the Photosensitive Pigment Prussian Blue. *J. Raman Spectrosc.* **2018**, *49*, 1198–1204. [CrossRef]
31. Osticioli, I.; Mendes, N.F.C.; Nevin, A.; Gil, F.P.S.C.; Becucci, M.; Castellucci, E. Analysis of Natural and Artificial Ultramarine Blue Pigments Using Laser Induced Breakdown and Pulsed Raman Spectroscopy, Statistical Analysis and Light Microscopy. *Spectrochim. Acta Part A Mol. Biomol. Spectrosc.* **2009**, *73*, 525–531. [CrossRef]
32. Scheuermann, W.; Ritter, G.J. The Vibrational Spectra of Strontium Chromate (SrCrO4) and Lead Chromate (PbCrO4). *Z. Naturforsch. A* **1970**, *25*, 1856–1862. [CrossRef]
33. Frost, R.L. Raman Microscopy of Selected Chromate Minerals. *J. Raman Spectrosc.* **2004**, *35*, 153–158. [CrossRef]
34. Errandonea, D.; Muñoz, A.; Rodríguez-Hernández, P.; Proctor, J.E.; Sapiña, F.; Bettinelli, M. Theoretical and Experimental Study of the Crystal Structures, Lattice Vibrations, and Band Structures of Monazite-Type $PbCrO_4$, $PbSeO_4$, $SrCrO_4$, and $SrSeO_4$. *Inorg. Chem.* **2015**, *54*, 7524–7535. [CrossRef]
35. Košařová, V.; Hradil, D.; Hradilová, J.; Čermáková, Z.; Němec, I.; Schreiner, M. The Efficiency of Micro-Raman Spectroscopy in the Analysis of Complicated Mixtures in Modern Paints: Munch's and Kupka's Paintings under Study. *Spectrochim. Acta Part A Mol. Biomol. Spectrosc.* **2016**, *156*, 36–46. [CrossRef]
36. Xu, J.F.; Ji, W.; Shen, Z.X.; Li, W.S.; Tang, S.H.; Ye, X.R.; Jia, D.Z.; Xin, X.Q. Raman Spectra of CuO Nanocrystals. *J. Raman Spectrosc.* **1999**, *30*, 413–415. [CrossRef]
37. Debbichi, L.; Marco De Lucas, M.C.; Pierson, J.F.; Krüger, P. Vibrational Properties of CuO and Cu 4O 3 from First-Principles Calculations, and Raman and Infrared Spectroscopy. *J. Phys. Chem. C* **2012**, *116*, 10232–10237. [CrossRef]
38. Basso, E.; Invernizzi, C.; Malagodi, M.; La Russa, M.F.; Bersani, D.; Lottici, P.P. Characterization of Colorants and Opacifiers in Roman Glass Mosaic Tesserae through Spectroscopic and Spectrometric Techniques. *J. Raman Spectrosc.* **2014**, *45*, 238–245. [CrossRef]
39. Platania, E.; Streeton, N.L.W.; Vila, A.; Buti, D.; Caruso, F.; Uggerud, E. Investigation of Mineralization Products of Lead Soaps in a Late Medieval Panel Painting. *Spectrochim. Acta Part A Mol. Biomol. Spectrosc.* **2020**, *228*, 117844. [CrossRef] [PubMed]
40. Ghervase, L.; Cortea, I.M. Lighting Up the Heritage Sciences: The Past and Future of Laser-Induced Fluorescence Spectroscopy in the Field of Cultural Goods. *Chemosensors* **2023**, *11*, 100. [CrossRef]
41. Cucci, C.; Delaney, J.K.; Picollo, M. Reflectance Hyperspectral Imaging for Investigation of Works of Art: Old Master Paintings and Illuminated Manuscripts. *Acc. Chem. Res.* **2016**, *49*, 2070–2079. [CrossRef] [PubMed]
42. Le Ru, E.C.; Etchegoin, P.G. *Principles of Surface-Enhanced Raman Spectroscopy*; Elsevier: Amsterdam, The Netherlands, 2009; ISBN 978-0-444-52779-0.
43. Becucci, M.; Ricci, M.; Lofrumento, C.; Castellucci, E. Identification of Organic Dyes by Surface-Enhanced Raman Scattering in Nano-Composite Agar-Gel Matrices: Evaluation of the Enhancement Factor. *Opt. Quantum Electron.* **2016**, *48*, 449. [CrossRef]
44. Pozzi, F.; Leona, M. Surface-Enhanced Raman Spectroscopy in Art and Archaeology. *J. Raman Spectrosc.* **2015**, *47*, 67–77. [CrossRef]
45. Leona, M.; Decuzzi, P.; Kubic, T.A.; Gates, G.; Lombardi, J.R. Nondestructive Identification of Natural and Synthetic Organic Colorants in Works of Art by Surface Enhanced Raman Scattering. *Anal. Chem.* **2011**, *83*, 3990–3993. [CrossRef]

46. Leona, M. Microanalysis of Organic Pigments and Glazes in Polychrome Works of Art by Surface-Enhanced Resonance Raman Scattering. *Proc. Natl. Acad. Sci. USA* **2009**, *106*, 14757–14762. [CrossRef]
47. Platania, E.; Lombardi, J.R.; Leona, M.; Shibayama, N.; Lofrumento, C.; Ricci, M.; Becucci, M.; Castellucci, E. Suitability of Ag-Agar Gel for the Microextraction of Organic Dyes on Different Substrates: The Case Study of Wool, Silk, Printed Cotton and a Panel Painting Mock-Up. *J. Raman Spectrosc.* **2014**, *45*, 1133–1139. [CrossRef]